



Babeş-Bolyai University
Cluj-Napoca
Faculty of Physics



Synthesis of Silver and Gold Nanoparticle Structures and Their Interaction with Molecules and Light

PhD Thesis Summary

PhD Candidate

Tóodor István Szabolcs

PhD Coordinator

Prof. Dr. Vasile Chiş

Babeş-Bolyai University

Cluj-Napoca, Romania

2019

Abstract

The present PhD thesis enriches the scientific world of nanomaterials by two newly developed colloidal nanoparticles structures. Beside their high Raman enhancing properties the chloride capped silver nanoparticles bring new insights regarding the fundamental principles of surface-enhanced Raman scattering (SERS), while our gold nanostructures are potential candidates for cancer photothermal therapy.

First, a short research background containing a succinct presentation of a wide range of nanostructures already existing in the literature is presented. It also mentions a discrepancy of the SERS mechanism regarding to the existence of the hot-spots, highlighting the need of new nanostructures which might help in the explanation of the fundamentals of SERS.

The first chapter describes the theory behind the techniques used for the experimental characterization of the newly developed nanostructures .

In chapter two the newly developed gold colloidal nanostructures are presented. The preparation of colloidal nanostructures in a one step procedure, reducing HAuCl_4 by hydroxylamine hydrochloride, without the use of any additional nucleating agent is described. This synthesis method has the advantage of preparation at room temperature. Moreover, the size of the nanoparticle assemblies (NPAs) is controllable in the 20-120 nm

range by stabilizing the colloid with bovine serum albumin (BSA) at different time moments after the synthesis. It is also presented the potential of colloidal nanoparticle assemblies to be used in cancer photothermal therapy by characterizing the cytotoxicity and the heat conversion capability of the gold NPAs.

In the third chapter the synthesis of a new stable colloidal solution of silver nanoparticles (AgNPs) capped only with chloride ions is described. This synthesis provides an already activated surface for electronic coupling between adsorbate and AgNPs surface which gives high intensity SERS spectra.

The last chapter presents an adatom model for SERS. It highlights that Raman enhancement originates from the electronic coupling of the analyte with the metal surface, mediated by specific ions that form SERS active sites on the surface of the nanoparticles. The spectra of anionic and cationic analytes can be recorded specifically by generating specific SERS active sites, obtained by adsorbed ions such as Ca^{2+} and Cl^- , respectively.

Keywords

Gold nanoparticles, nanoparticle assemblies, controllable size, hydroxylamine hydrochloride reduction, room temperature synthesis, albumin surface modification , photothermal effect, Raman mapping, phototherapeutic agent, chloride activation, electronic coupling, photoreduction, silver nanoparticles, SERS, SERS-active sites, SERS switch-on effect.

Contents of the PhD thesis

Abstract	5
Research Background and Motivation.....	7
Chapter I	
1. Theory and Methodology.....	11
1.1. Vibrational spectroscopy.....	11
1.1.1. IR and Raman spectroscopy.....	11
1.1.2. Surface-enhanced Raman spectroscopy.....	17
1.1.2.1. Electromagnetic enhancement.....	18
1.1.2.2. Chemical enhancement.....	19
1.1.2.3. SERS substrates.....	20
1.2. Principal component analyses.....	21
1.3. Biological evaluation methods.....	22
1.3.1. Cytotoxicity evaluation.....	22
1.3.2. Oxidative stress evaluation.....	24
1.4. Instrumentation.....	26
Chapter II	
2. Hydroxylamine-hydrochloride Reduced Gold Nanoparticles	28
2.1. Introduction.....	28
2.1.1. Materials.....	29

2.2. Nanoparticles synthesis.....	29
2.3. Physical and optical characterization of the gold NPAs..	31
2.4. Controllable sized gold nanoparticles.....	35
2.5. SERS enhancement of NPAs ²⁰	38
2.6. Biological evaluation.....	40
2.6.1. Cytotoxicity assay.....	41
2.6.2. Oxidative stress evaluation.....	43
2.7. Photothermal properties.....	45
2.7.1. Raman imaging.....	47
2.8. Conclusions	52
 Chapter III	
3. Chloride Capped Silver Nanoparticles.....	53
3.1. Introduction.....	54
3.1.1. Materials.....	54
3.2. Synthesis of the chloride capped silver nanoparticles.....	54
3.3. Physical and chemical properties of the Cl-AgNPs.....	56
3.4. SERS enhancement of Cl-AgNps.....	61
3.5. Conclusions.....	64
 Chapter IV	
4. The Adatom Approach of SERS Enhancement.....	65
4.1. Introduction.....	65

4.2. AgNps activation.....	66
4.3. Concentration dependent SERS active sites.....	71
4.4. Specific SERS detection.....	75
4.5. Conclusions.....	81
List of publication.....	82
Acknowledgments.....	83
References.....	84

Contents

Research Background and Motivation.....	9
1. Hydroxylamine-hydrochloride Reduced Gold Nanoparticles	12
2. Chloride Capped Silver Nanoparticles.....	19
3. The Adatom Approach of SERS Enhancement.....	24
4. Conclusions.....	31
5. Publications	
5.1. Scientific Articles.....	34
5.2. Articles Sent for Publication.....	36
5.3. Conference Poster Presentations.....	36
6. References.....	37

Research Background and Motivation

In the 21st century nanotechnology is part of our life. One of the biggest areas of nanotechnology is the nanoparticles synthesis which has become an important multidisciplinary research due to its great variety of applicability.

Medical technologies are constantly developing, thus nanoparticles might be used to improve or replace today's therapies or diagnoses. The major advantage of the nanoparticles compared to ordinary techniques is that they can be engineered to have certain properties. Early diagnosis is critical to ensure early treatment and thus a better chance for curing a disease, particularly diseases like cancer. One of the greatest interest found at the border of biophysics, nanotechnology and nanomedicine is related to noble metal nanoparticles, particularly silver and gold, due to their special chemical and optical properties [1, 2], which enable a good control regarding dimension, shape, surface functionalization [3] and biocompatibility [4]. Metallic nanoparticles have been used for non-invasive cancer detection [5], as drug agents [6], as drug delivery vehicles [7], for photothermal therapy [8], as contrast agents [9] or as surface-enhanced Raman scattering spectroscopy surfaces [10].

Raman spectroscopy represents an emerging technique for life-science applications. The great potential of Raman spectroscopy resides in the rich molecular information provided by the method

and in the general high sensitivity of SERS. Despite of an increasing number of SERS studies in a wide range of research areas, the origin of the high enhancement is still not understood completely. There are two widely accepted mechanisms which are responsible for the high SERS enhancement. One of them is the electromagnetic enhancement based on the excitation of localized surface plasmons [11]. The other is the chemical enhancement based on a charge transfer effect [12]. In case of extremely high enhancement, single molecule levels, the SERS effect is also explained by the formation of electromagnetic hot-spots generated by aggregated nanoparticles [13]. Some inconsistencies of the hot-spot model was stated by Otto and his coworkers and an adatom model has been proposed [14-17]

Even though the SERS question is not solved, engineered nanomaterials are necessary which can grant us new physical, chemical and biological properties. Nanoparticles can assemble either in an organized manner, according to a predetermined pattern, or randomly. Beside controlled geometry, self-organized three-dimensional superstructures [18, 19], anisotropic hybrid metal nanostructures, like gold and silver nano-stars [20], or flower shaped nanoparticles [21] have proven their utility .

Synthesis and biomedical applications of popcorn like shaped nanoparticles have been reported recently by Lu et al. [22, 23]. The popcorn shaped gold nanoparticles were synthesized using a seed-mediated growth procedure in the presence of cetyl trimethylammonium bromide (CTAB). It was found that the

aggregation of nanoparticles on cancer cells surface leads to absorption in the near infrared (NIR) region. Thus, the applicability of the popcorn gold nanoparticles for photothermal therapy was assessed.

Photothermal therapy is a new promising weapon against cancer. During the irradiation of the cancer cells with light in the NIR region the surface plasmon resonance property of the nanoparticles convert the electromagnetic waves into heat which causes changes in the cell physiology, thus death of the cells.

A great number of nanostructures are already available for different fields of interest but there is still space and need for the developments of newer ones. The thesis contains newly prepared gold colloidal nanostructures with controllable size by reducing in a one step procedure HAuCl_4 by hydroxylamine hydrochloride without the use of any additional nucleating agent. The potential of these colloidal nanostructures to be used as photothermal therapy agents were also studied. It also describes novel chloride activated silver nanoparticles by silver chloride photoreduction. These nanoparticles facilitate the reliable detection of molecules at low concentrations and brings new insights regarding the fundamental principles of surface-enhanced Raman scattering.

1. Hydroxylamine-hydrochloride Reduced Gold Nanoparticles

The newly developed gold nanostructures were synthesized by the reduction of Au^{3+} in the presence of hydroxylamine hydrochloride. A slight change in the addition order of the reactants led to nanoparticles assemblies of different size. The two type of nanoparticles were named NPAs20 and NPAs120 after their mean size diameter. The two sets of nanoparticles have different morphological and optical properties. **Figure 1.1** shows the UV-Vis absorption spectra of the two colloids, while on **Figure 1.2**. their morphology is presented.

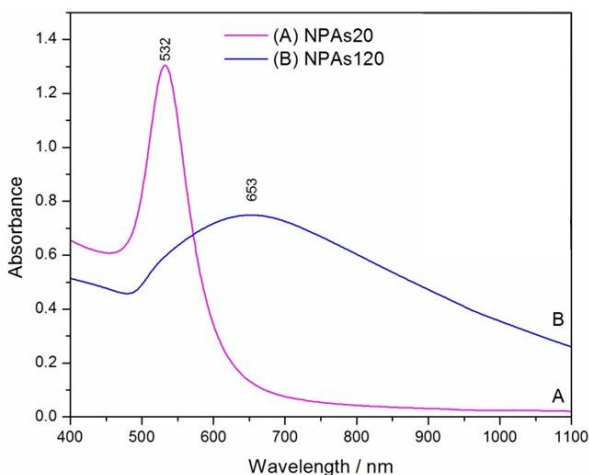


Figure 1.1. UV-Vis spectra of NPAs20 (A) and NPAs120 colloids (B) recorded one day after preparation.

The two colloids require a stabilization time, therefore the absorption maximum of the prepared colloids was measured one day after synthesis. UV-Vis absorption maximum positions and bands width of colloids predicts that the NPAs120 colloid, with an absorption maximum at 653 nm, contains nanostructures of larger diameter and broader size distribution than those in the NPAs20 colloid, which shows an absorption maximum at 532 nm.

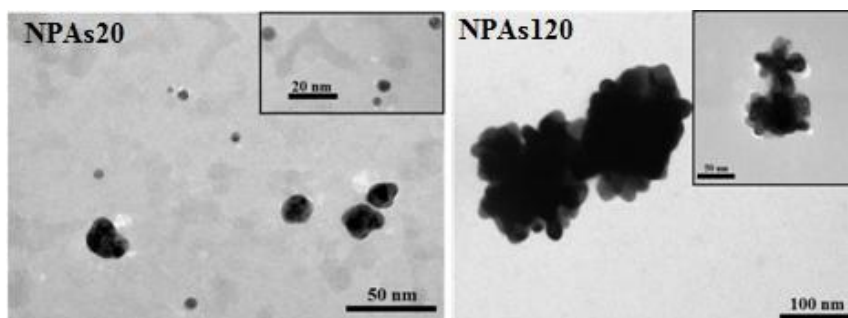


Figure 1.2. Transmission electron microscopy (TEM) images of NPAs20 (Left) and NPAs120 (Right).

The TEM images of the NPAs20 colloid show heterogeneous structures of 10-35 nm in diameter, but also smaller nanoparticles with diameters of 4-8 nm, while the NPAs120 colloid consist of irregular, popcorn-like nanostructures with a broad size distribution in the 80-140 nm range

As it was mentioned before, the two colloids requires a stabilization time. Right after mixing the reagents and synthesis of the colloids, large assemblies are formed, which break in smaller

ones in the timeline of a day. By the addition of bovine serum albumin (BSA) during the natural fragmentation process the nanoparticle assemblies can be controlled in the 20-120 nm range.

The high SERS activity of the newly developed gold colloidal NPAs, where proven by comparative SERS measurements using the hydroxylamine and conventional citrate [24] reduced gold nanostructures and three different test molecules. The results are

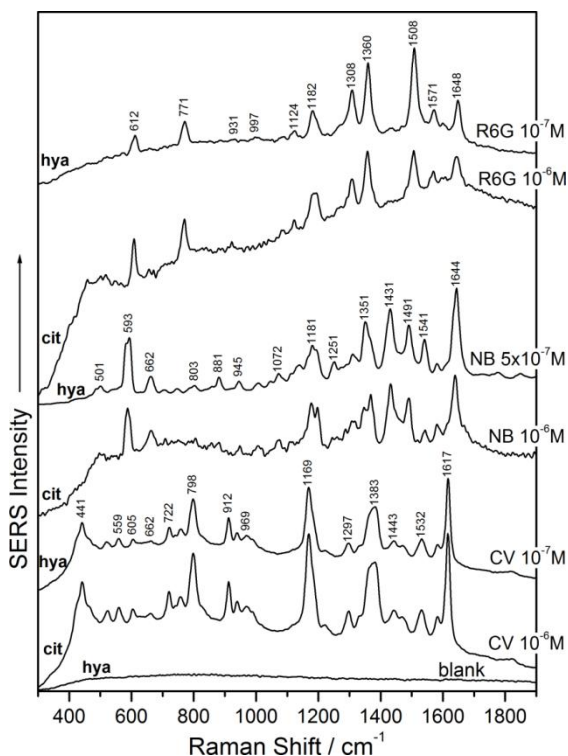


Figure 1.3. SERS spectra of Crystal Violet, Nile Blue and Rhodamine 6G obtained by using hydroxylamine (hya) and citrate (cit) reduced gold colloids

shown on **Figure 1.3**. The obtained SERS spectra have similar quality in case of both colloids, but the analyte concentration in case of the hydroxylamine reduced colloid was 10 times lower.

In order to use nanomaterials in living cells their biocompatibility must be tested. The cytotoxicity of AuNPs depends on several factors, including their size, shape and surface chemistry [25, 26]. The cytotoxic effect of NPAs was evaluated by using the MTT assay, which is based on the enzymatic reduction of yellow MTT reagent to purple formazan crystals only by metabolically active human lung adenocarcinoma (A549) cells. The results were expressed as percent survival compared to untreated controls and are presented on **Figure 1.4**.

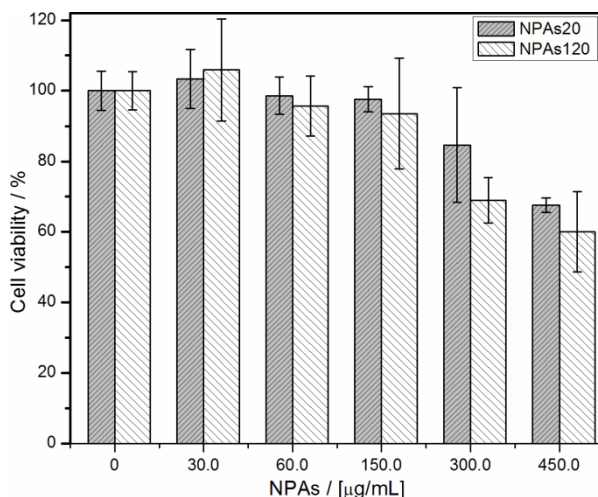


Figure 1.4. Cell viability of A549 cells exposed to NPAs20 and NPAs120 in concentrations ranging from 30 to 450 µg/mL for 24 h.

The data shows that NPAs induce a significant decrease in cell viability only at higher gold concentrations (300 or 450 $\mu\text{g/mL}$). Compared to NPAs20, NPAs120 presented increased cytotoxicity, but the differences in cell viability were within 5% at concentrations below 150 $\mu\text{g/mL}$. A previous study involving gold nanoshell-mediated photothermal therapy in a murine glioma model has found that a blood concentration of 100 $\mu\text{g/g}$ of gold is enough for determining significant responses after irradiation [27].

After the biocompatibility test the possibility of the hydroxylamine reduced gold NPAs to be used as photothermal therapy agents was probed, by testing their light to heat conversion capability. The light-to-heat conversion capability of NPAs was measured by monitoring the rise in temperature of the concentrated colloids due to laser irradiation. For the irradiation two different laser wavelengths (532 nm and 785 nm) were used comparatively.

It was found that the NPAs120 convert light energy to heat more effectively than the NPAs20 in case of both used wavelengths, due to the presence of a broad plasmonic resonance band centered around 653 nm (see **Figure 1.1.**). The NPAs120 reached a maximum temperature of 57.6 $^{\circ}\text{C}$ with the 785 nm laser and 43.6 $^{\circ}\text{C}$ with the 532 nm lasers while the NPAs20 reached a maximum temperature of 39.6 $^{\circ}\text{C}$ with the 532 nm laser and just 33.9 $^{\circ}\text{C}$ with the 785 nm laser. The use of the 785 nm laser is advantageous especially for *in vivo/ex vivo* applications, due to the fact that it matches the therapeutic window between 650 nm

and 1350 nm where the NIR light has maximum tissue depth penetration.

Since validating the use of NPAs as photothermal agents *in vivo* requires the use of lasers, Raman mapping was implemented. Raman imaging was used to detect the damage inflicted by NPAs photothermal effect on cells upon laser irradiation. The spectral data was analyzed using principal component analysis (PCA). **Figure 1.5.** shows the cells before and after irradiation and also the corresponding Raman map based on PCA.

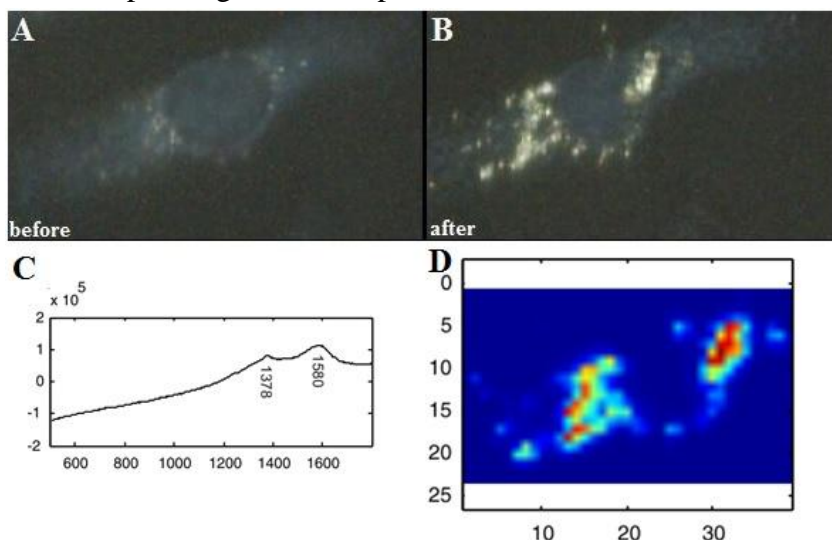


Figure 1.5. Representative microscopy images obtained by dark field microscopy images before (A) and after (B) the irradiation and the score plots of the Raman map (D) and the corresponding loading plot (C).

The Raman spectra of the cells show bands at 1378 cm^{-1} and 1580 cm^{-1} representing the D and G bands of carbon materials, which

are byproducts of thermal damage [28]. According to **Figure 1.5.**, the red areas in the score plots depict regions with intense thermal damage. When compared to dark field images of the same cell, we observe an overlap between those red areas and the large clusters of NPAs120. Thus, it can be concluded that the NPAs are directly responsible for the thermal degradation in the cell.

2. Chloride Capped Silver Nanoparticles

For the preparation of the new chloride capped silver colloidal solution (Cl-AgNPs), the reagent were added in a beaker and then were exposed to the light of a conventional reading-lamp equipped with a commercial LED bulb, under constant magnetic stirring . **Figure 2.1.** picture (A) shows the experimental setup of the Cl-AgNPs synthesis while picture (B) shows the prepared colloid.

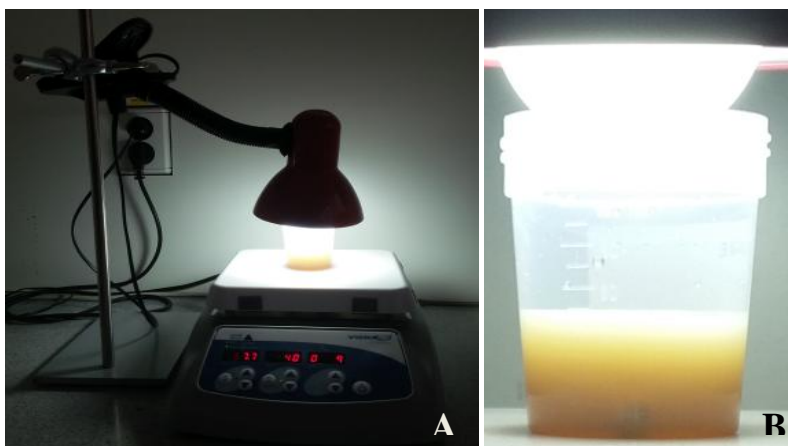


Figure 2.1. Picture (A) shows the experimental arrangement for the synthesis of Cl-AgNPs. A desk lamp with an LED bulb was placed above the beaker containing the reaction mixture. Picture (B) shows the colloidal solution of Cl-AgNPs obtained after 10 min of light exposure.

After three minutes of light exposure, the transparent solution turned pale yellow. The further change in the color of the solution

to an intense gray-brown after 5 min of light exposure indicated a high concentration of AgNPs in the solution.

Photoreduction of silver nanoparticles is already reported in the literature. In most of the reported studies the photosynthesis was performed in the presence of organic stabilizing agents such as citrate [29] or poly(*N*-vinylpyrrolidone) [30, 31]. Compared to these studies, the most important novelty of our protocol is represented by the rapid synthesis in addition to the absence of any organic capping agent.

Mixing the silver nitrate and sodium chloride in the reacting solution resulted in the generation of a flocculent precipitate of AgCl. The presence of AgCl particles in the solution was evidenced in the UV–Vis spectra as an intense absorption band at 254 nm (**Figure 2.2.**). During the synthesis the photoconversion of AgCl microparticles to AgNPs was monitored by UV-Vis spectroscopy and is presented in **Figure 2.2.** During light exposure, the intensity of the 254 nm band due to AgCl absorption decreases as AgNPs are formed, whereas the intensity of the silver plasmon band at 429 nm increases. During the photoreduction process, the surface of the AgCl particles becomes covered with clusters of Ag atoms, which was also reported by Wang et al. [32]. The silver atom clusters grow continuously during light exposure, leading to the formation of AgNPs on the surface of AgCl microparticles. After 5 min of light exposure, the plasmon resonance band became narrower, showing a typical shape for silver colloids.

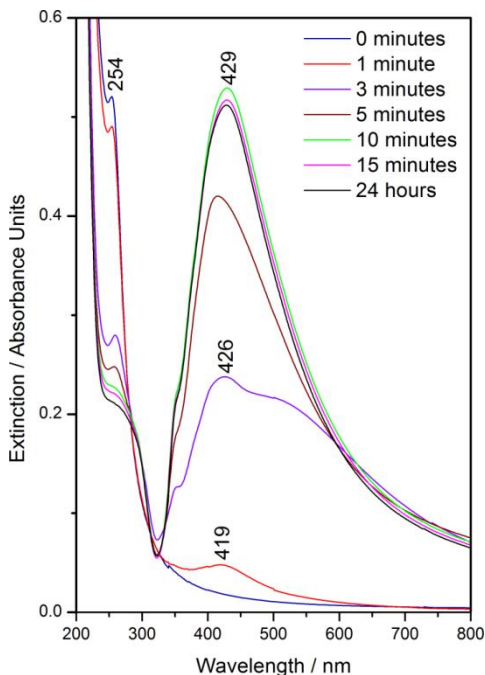


Figure 2.2. UV–Vis extinction spectra obtained during the Cl-AgNP synthesis, recorded after 0, 1, 3, 5, 10 and 15 min of light exposure to the reacting mixture in addition to 24 h after the colloid synthesis.

Between 5 and 10 min of light exposure, the intensity of the plasmonic band at 429 nm reaches its maximum, and no further increase of the plasmonic band intensity could be observed between 10 and 15 min of light exposure. The size of the AgNPs shows polydispersity with diameters in the 10-80 nm range and various geometries such as spherical, polyhedral or rods. The shape polydispersity could be a result of the lack of an organic surfactant. It is known that nanoparticles with geometries with

sharp curvatures lead to intense field enhancement and thus to a high Raman scattering enhancement. In order to highlight the SERS enhancement capability of the newly developed Cl-AgNPs, comparative measurements using trisodium citrate reduced silver nanoparticles (cit-AgNPs) and hydroxylamine hydrochloride reduced silver nanoparticles (hya-AgNPs) were performed, using crystal violet chloride as test analyte. The results of the SERS measurement are shown in **Figure 2.3**.

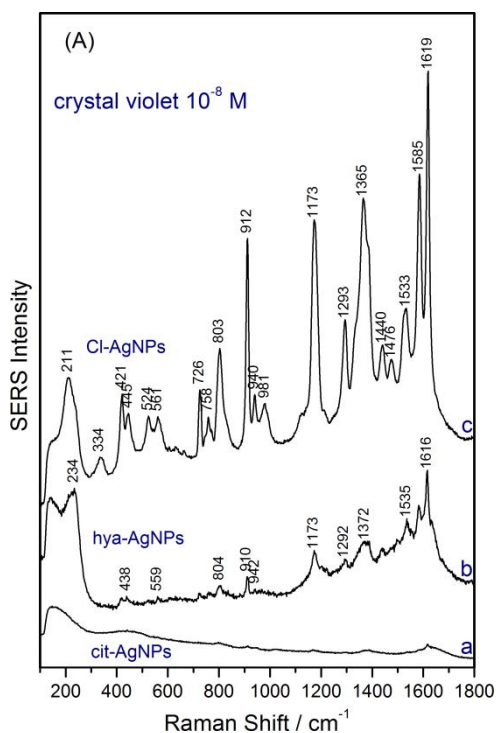


Figure 2.3. SERS spectra of 10^{-8} M crystal violet by using cit-AgNPs (a), hya-AgNPs (b) and Cl-AgNPs (c) as SERS substrate.

As it can be observed in **Figure 2.3.**, the Cl-AgNPs as SERS substrate leads by far to the highest intensity of crystal violet. This can be explained within the adatom model, by the high concentration of Cl^- anions, which lead to the electronic coupling between adsorbate and metal silver surface. The chemisorbed Cl^- ions mediate the electronic coupling of the cationic molecules by forming Cl^- -adsorbate surface complexes [33], forming SERS-active sites on the AgNPs. Thehya-AgNP colloid contains a much lower number of Cl^- anions, which are present in the solution because of the hydrochloride salt of hydroxylamine. Thus, only a limited number of SERS active sites are available due to the presence of Cl^- ions, which explain the low intensity SERS spectra of crystal violet. When using the cit-AgNP colloid as SERS substrate, no spectra could be obtained at the tested concentration. However, after adding 0.1 M NaCl to the cit-AgNP colloid, high intensity SERS spectra could be obtained, which are of comparable intensity with those obtained with Cl-AgNPs as substrate.

3. The Adatom Approach of SERS Enhancement

Chloride anions are often added to metal colloids to enhance the Raman signal. When the SERS effect is explained in terms of the electromagnetic mechanism, an aggregation effect of the colloidal nanoparticles is attributed to the chloride ions. Nanoparticle aggregates, particularly near the gap sites between two particles in proximity, can lead to the formation of electromagnetic hot spots – sites with highly increased field strengths. It is still unclear why the other component molecules in the solutions are not enhanced due to the hot-spots.

Another explanation for the high SERS enhancement obtained after the addition of Cl^- ions is that new SERS active sites are generated. The creation of SERS active sites by chloride-activation can be explained in the adatom model, proposed by Otto and co-workers, by the formation of stable chloride-molecular adsorbate surface complexes, which facilitate the charge-transfer enhancement mechanism .

Herein it is presented that by the use of proper adatoms SERS signals of different analytes can be improved and that the aggregation of the nanoparticles, and thus formation of the hot-spots are not necessary for high SERS enhancement.

During the synthesis of SERS substrates the used reagents are in range of mM concentration therefore the normal Raman spectroscopy is not sensitive enough to observe any distinct peaks of the substrates. The surfactant used for the synthesis prohibits

the aggregation of nanoparticles via electronic repulsions between the nanoparticles. If there is no electronic coupling between the metallic surface and the surfactant then the latter does not generate any SERS spectrum. Under certain conditions, when the surfactant adsorbs to the AgNP and becomes in a chemical contact with the surface, the surfactant exhibits intense SERS spectra. The Raman spectrum of the blank colloids in comparison with water can be seen in **Figure 3.1**.

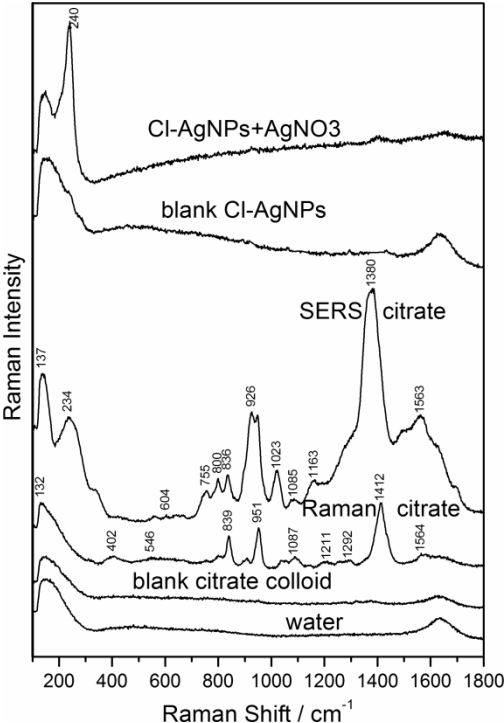


Figure 3.1. Raman spectrum of water, Raman spectrum of the silver colloidal solution obtained by reduction with citrate, Raman spectrum of 1 M citrate,

SERS spectrum of citrate obtained after addition of AgNO_3 to the silver colloid, blank Raman spectrum of Cl-AgNPs colloidal solution, SERS spectrum of Cl-AgNPs colloidal solution showing the Ag-Cl band after addition of AgNO_3 to the silver colloid.

The SERS intensity of an analyte can be increased by adding cations such as Ag^+ , Mg^{2+} or Ca^{2+} . Thus, the addition of Ag^+ cations to the citrate colloid facilitates the forming of Ag^+ -citrate complexes at the nanoparticle silver surface, involving a chemical bond between the adsorbate and silver substrate. **Figure 3.1.** shows the obtained intense citrate SERS spectrum after the addition of AgNO_3 . The intense band at 234 cm^{-1} indicates the interaction of Ag^+ -citrate anion complex with the silver surface, the 234 cm^{-1} band being assigned to a Ag-O stretching vibration.

Similarly in case of AgCl colloid the Ag-Cl^- vibration is missing, suggesting an electrostatic interaction between the chloride ions and the silver surface. By adding AgNO_3 to the already prepared colloidal solution, an intense peak at 240 cm^{-1} is clearly visible, assigned to Ag-Cl vibration. Thus, the chloride ion adsorbs to the silver surface mediated by the Ag^+ ions and forms Ag^+ - Cl^- surface complexes, in line with the adatom model.

The lack of SERS-active sites in the cit-AgNPs allows the observation in an instructive manner of the SERS switch effect after SERS activation of colloid and the coupling of the analyte to the silver surface. **Figure 3.2** shows the Cit-AgNPs activation.

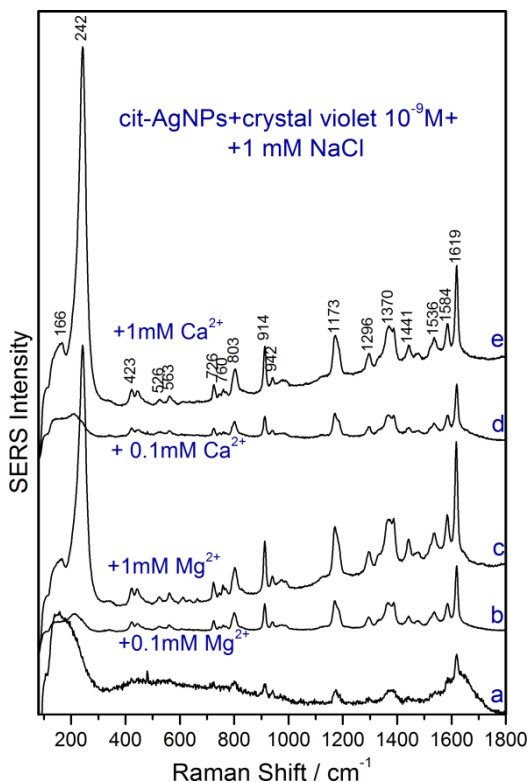


Figure 3.2. SERS spectra of 10^{-9} M crystal violet recorded using the cit-AgNPs as substrates. cit-AgNPs+1mM NaCl (a), cit-AgNPs+1mM NaCl and 10^{-4} M MgSO_4 (b), cit-AgNPs+1mM NaCl and 1 mM MgSO_4 (c), cit-AgNPs+1mM NaCl and 10^{-4} M $\text{Ca}(\text{NO}_3)_2$ (d), cit-AgNPs+1mM NaCl and 1 mM $\text{Ca}(\text{NO}_3)_2$ (e).

The cit-AgNPs did not allow the recording of SERS bands of crystal violet at 10^{-9} M concentration, so the addition of 1 mM NaCl was needed to activate the cit-AgNPs. The presence of 1 mM Cl^- led only to a weak activation of the cit-AgNPs (spectrum

a). However, the further addition of cations in concentrations ranging from 10^{-4} – 10^{-3} M to a cit-AgNP solution which already contains 1 mM NaCl, led to the switching on of the SERS effect and the recording of very intense SERS spectra of 10^{-9} M crystal violet. Moreover, a further raise in intensity of the SERS spectra of crystal violet can be observed by increasing the concentration of Mg^{2+} or Ca^{2+} ions to 1 mM in the case of cit-AgNPs which were previously activated by adding 1 mM NaCl. The intensity of the SERS spectrum of an analytes at a given concentration depends on concentration of SERS active sites inside the used substrate.

It was already shown that by the addition of cations to the citrate reduced silver colloid the SERS spectrum of the citrate can be obtained (**Figure 3.3.**, spectrum b). The Ca^{2+} adions turn on the SERS effect, by mediating the chemisorption of citrate to the metallic silver surface. After the addition, of NaCl 10^{-3} M to the same colloidal solution, the SERS spectrum of citrate completely disappears, and the SERS spectrum of Ag-Cl appears indicated by a band at 242 cm^{-1} (spectrum c). The selective adsorption of citrate and chloride can be explained by their different affinities for the nanoparticle silver surface. The affinity of the Cl^- is stronger than the affinity of the citrate for silver surfaces, therefore, Cl^- can easily replace citrate from the SERS specific sites. Since the added salts were in low concentration the appearance of spectra due to aggregation was excluded. The colloids were found to be stable for weeks.

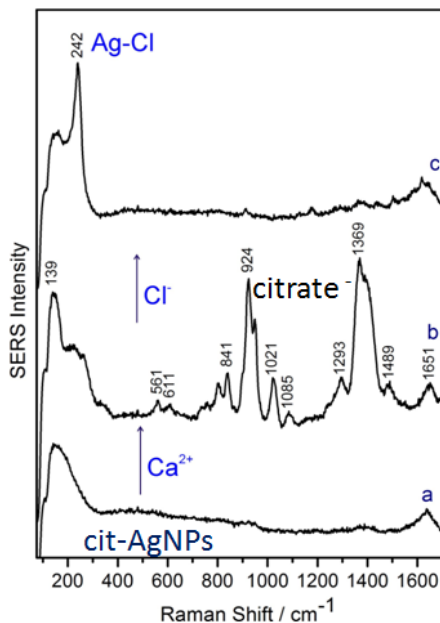


Figure 3.3. Specific SERS turn on of citrate after activation of cit-AgNPs with Ca^{2+} and Cl^- , respectively: (a) Raman blank spectrum of the cit-AgNPs (b) SERS spectrum of citrate obtained by the addition of Ca^{2+} to the cit-AgNPs, (c) SERS spectrum cit-AgNPs obtained after addition of Cl^- to the cit-AgNPs.

The specific SERS detection was further studied by using CV as test analytes. The spectral table in **Figure 3.4.** contains spectra recorded from the same crystal violet 10^{-8} M in cit-AgNPs solution, modified by sequentially adding Ca^{2+} and Cl^- . The SERS spectrum of crystal violet 10^{-8} M with cit-AgNPs is blank (spectrum a). When to the same solution, $\text{Ca}(\text{NO}_3)_2$ 10^{-4} M is added, the recorded spectrum shows the citrate SERS bands (, spectrum b), indicating that the Ca^{2+} SERS active sites promote the chemisorption of citrate anions.

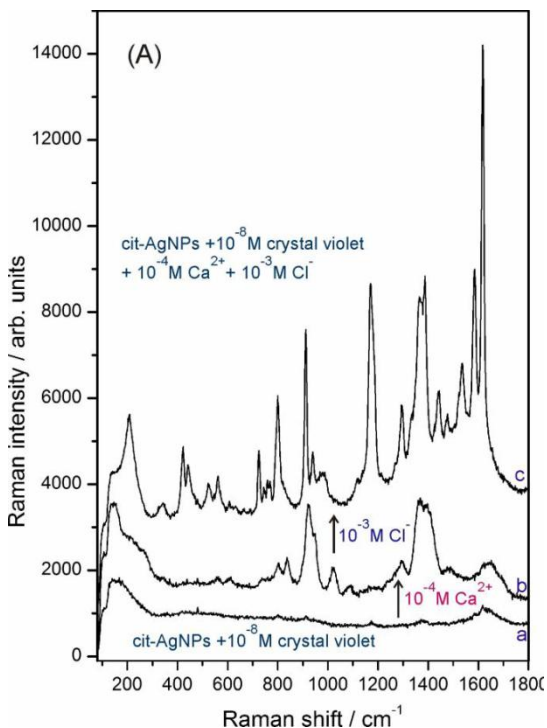


Figure 3.4. Specific SERS detection of citrate anion and CV cationic dye by SERS activation of the cit-AgNPs with Ca^{2+} and Cl^- , respectively. Blank spectrum obtained for CV 10^{-8} M in cit-AgNPs (a), SERS spectrum of citrate after activation of the colloid with Ca^{2+} (b), SERS spectrum of CV after addition of Cl^- (c);

Next, when $\text{NaCl } 10^{-3}$ M is added to the same solution, the SERS bands of citrate disappear, while the SERS bands of crystal violet 10^{-8} M appear (spectrum c). Thus, the Cl^- ions, due to their higher affinity for the silver surface, replace the citrate anions from the Ca^{2+} SERS active sites, forming now Cl^- SERS active sites for crystal violet.

4. Conclusions

A new, effective and simple procedure for preparing gold nanoassemblies with mean diameters of 20 and 120 nm based on reduction with hydroxylamine hydrochloride has been described. All prepared colloids were found to be stable at least for two months. The 120 nm nanoassemblies show absorption in the NIR spectral region, a feature which provides them potential for photothermal application.

By surface modification with bovine serum albumin at different time moments after synthesis, highly stable nanoparticle assemblies of controllable dimension can be obtained.

SERS spectra at 10^{-7} M analyte concentration were recorded using hydroxylamine reduced nanoassemblies as substrate, showing a better SERS enhancement property, compared to conventional citrate reduced colloidal nanoparticles.

NPAs are well tolerated by the A549 cells until a concentration of 300 $\mu\text{g/mL}$.

In terms of their photothermal capabilities, the NPAs120 were found to convert light energy to heat more effectively than the NPAs20 especially when irradiated with the 785 nm laser, due to their broad plasmonic band centered at 650 nm.

We demonstrated that Raman spectroscopy can effectively highlight the cellular damage due to photothermal effect, by identifying characteristic Raman bands of intracellular carbon

byproducts. The carbon byproduct deposits were found to overlap with the intracellular regions that were rich in nanoparticles. These results highlight that the NPAs obtained by hydroxylamine reduction are potential candidates for nanoparticle based photothermal therapy.

Synthesis methodology for chloride capped AgNPs obtained through AgCl photoconversion was described. A simple and efficient method adopted in our lab consists of irradiating the reaction mixture for 5-10 minutes and subsequent overnight storage.

Compared to conventional silver nanoparticles, the Cl-AgNPs are advantageous due to the presence of a single chloride capping agent, leading to a clean surface from a SERS spectroscopic point of view. This strategy prevents the occurrence of artifacts, due to the adsorption to the silver surface of organic reaction products.

The Cl-AgNPs show very intense SERS spectra of cationic analytes due to the formation of charge transfer complexes with the silver metal surface.

It was shown that the SERS effect is turned on by the presence of SERS active sites on the silver nanoparticle surface. To sustain the adatom theory, we showed that the SERS spectrum of anions such as citrate or Cl^- can be recorded mediated by cations such as Ag^+ or Mg^{2+} , in accordance with the adatom model. In the presence of multiple anions in the solution, the adsorption to the silver surface occurs in the sequence of their surface contact adsorption strength. This also shows that the high surface enhancements might appear due to the increased number of SERS

active sites and not due to the aggregation of silver nanoparticles. In the adatom approach, the aggregation of the nanoparticles is an unnecessary step that rather contributes to the low reproducibility of SERS spectra.

Furthermore, the SERS effect is a specific end selective phenomenon in which for the detection of anionic species the addition of cationic adions whereas, for the cationic species the addition of anionic adions are needed in order to form specific SERS active sites.

Finally, the intensity of the SERS spectra is proportional with the number of the existing SERS active sites.

5.1. Scientific Articles

- Todor, Istvan Sz**, Szabo, Laszlo, Marisca, Oana T., Chis, Vasile, & Leopold, Nicolae. (2014). Gold nanoparticle assemblies of controllable size obtained by hydroxylamine reduction at room temperature. *Journal of Nanoparticle Research*, 16(12).
- Leopold, Nicolae, Stefanu, Andrei, Herman, Krisztian, **Todor, Istvan Sz.**, Iancu, Stefania D., Moisoiu, Vlad, & Leopold, Loredana F. (2018). The role of adatoms in chloride-activated colloidal silver nanoparticles for surface-enhanced Raman scattering enhancement. *Beilstein Journal of Nanotechnology*, 9, 2236-2247.
- Boitor, R. A., **Todor, I. Sz**, Leopold, L. F., & Leopold, N. (2015). Room Temperature Synthesis of Highly Monodisperse and Sers-Active Glucose-Reduced Gold Nanoparticles. *Journal of Applied Spectroscopy*, 82(3), 415-419.
- Leopold, Loredana Florina, **Todor, Istvan Szabolcs**, Diaconeasa, Zorita, Rugina, Dumitrita, Stefanu, Andrei, Leopold, Nicolae, & Coman, Cristina. (2017). Assessment of PEG and BSA-PEG gold nanoparticles cellular interaction. *Colloids and Surfaces a-Physicochemical and Engineering Aspects*, 532, 70-76.
- Magyari, Klara, One, Roxana, **Todor, Istvan-Szabolcs**, Baia, Monica, Simon, Viorica, Simon, Simion, & Baia, Lucian. (2016). Titania effect on the bioactivity of silicate bioactive glasses. *Journal of Raman Spectroscopy*, 47(9),

1102-1108.

- Pinzaru, S. Cinta, Muller, Cs., **Todor, I. S.**, Glamuzina, B., & Chis, V. (2016). NIR-Raman spectrum and DFT calculations of okadaic acid DSP marine biotoxin microprobe. *Journal of Raman Spectroscopy*, 47(6), 636-642.
- Szabo, Laszlo, Herman, Krisztian, Mircescu, Nicoleta Elena, **Todor, Istvan Szabolcs**, Simon, Botond Lorand, Boitor, Radu Alex, . . . Chis, Vasile. (2014). Surface-enhanced Raman scattering and DFT investigation of 1,5-diphenylcarbazine and its metal complexes with Ca(II), Mn(II), Fe(III) and Cu(II). *Journal of Molecular Structure*, 1073, 10-17.
- Marta, B.;Leordana,C.;**Istvan, T.**;Baritchi,R.; Astilean,S., Optimazition of various parameters for graphene synthesis by thermal chemical vapor deposition (CVD) on copper substrate., *Studia Universitatis Babes-Bolyai, Physica* . Dec2014, Vol. 59 Issue 2, p35-45. 11p
- Bogdan Marta, Cosmin Leordean, **Todor Istvan**, Ioan Botiz, Simion Astilean, Efficient etching-free transfer of high quality, large-area CVD grown graphene onto polyvinyl alcohol films, *Applied Surface Science*, Volume 363, 2016, Pages 613-618,

5.2. Articles Sent for Publication

István Sz Tódor, Oana Marisca, Dumitrita Rugina, Zorita Diaconeasa, Loredana Leopold, Cristina Coman, Elisabeta Antonescu, Zoltán Bálint, László Szabó, Stefania Iancu, Vasile Chis, Nicolae Leopold. (2019). Photothermal property assessment of gold nanoparticle assemblies obtained by hydroxylamine reduction

5.3. Conference Poster Presentations

Highly SERS Active Gold Nanoparticles Assemblies of Controllable Size, 8th International Conference on Vibrational Spectroscopy (ICAVS), 2015 Vienna, Austria

Preparation and Spectroscopic Characterization of Heparin-reduced Gold Nanoparticles at Room Temperature, 5th Conference on Advanced Spectroscopies on Biomedical and Nanostructured Systems (BIONANOSPEC), 2014 Cluj-Napoca, Romania

Synthesis of Popcorn Shaped Nanoparticle Assemblies, TIM13 International Physics Conference, 2013 Timisoara, Romania

Popcorn Shaped Gold Nanoparticles with Absorbance in NIR, The 5th National Conference of Applied Physics, CNFA 2013, Iasi, Romania

6.References

1. Qian, X., et al., *In vivo tumor targeting and spectroscopic detection with surface-enhanced Raman nanoparticle tags*. Nature Biotechnology, 2008. **26**(1): p. 83-90.
2. Lee, K.S. and M.A. El-Sayed, *Gold and silver nanoparticles in sensing and imaging: Sensitivity of plasmon response to size, shape, and metal composition*. Journal of Physical Chemistry B, 2006. **110**(39): p. 19220-19225.
3. Sperling, R.A. and W.J. Parak, *Surface modification, functionalization and bioconjugation of colloidal inorganic nanoparticles*. Philosophical Transactions of the Royal Society A: Mathematical, Physical and Engineering Sciences, 2010. **368**(1915): p. 1333-1383.
4. Dreaden, E.C., et al., *The golden age: gold nanoparticles for biomedicine*. Chemical Society Reviews, 2012. **41**(7): p. 2740-2779.
5. Lin, D., et al., *Colorectal cancer detection by gold nanoparticle based surface-enhanced Raman spectroscopy of blood serum and statistical analysis*. Optics Express, 2011. **19**(14): p. 13565-13577.
6. Pan, Y., et al., *Gold nanoparticles of diameter 1.4 nm trigger necrosis by oxidative stress and mitochondrial damage*. Small, 2009. **5**(18): p. 2067-76.
7. Iyer, A.K., et al., *Exploiting the enhanced permeability and retention effect for tumor targeting*. Drug Discovery Today, 2006. **11**(17-18): p. 812-818.
8. Dickerson, E.B., et al., *Gold nanorod assisted near-infrared plasmonic photothermal therapy (PPTT) of squamous cell carcinoma in mice*. Cancer Lett, 2008. **269**(1): p. 57-66.
9. Mornet, S., et al., *Magnetic nanoparticle design for medical applications*. Progress in Solid State Chemistry, 2006. **34**(2-4): p. 237-247.

10. Nie, S. and S.R. Emory, *Probing Single Molecules and Single Nanoparticles by Surface-Enhanced Raman Scattering*. Science, 1997. **275**(5303): p. 1102-1106.
11. Jeanmaire, D.L. and R.P. Van Duyne, *Surface raman spectroelectrochemistry: Part I. Heterocyclic, aromatic, and aliphatic amines adsorbed on the anodized silver electrode*. Journal of Electroanalytical Chemistry and Interfacial Electrochemistry, 1977. **84**(1): p. 1-20.
12. Albrecht, M.G. and J.A. Creighton, *Anomalously intense Raman spectra of pyridine at a silver electrode*. Journal of the American Chemical Society, 1977. **99**(15): p. 5215-5217.
13. Moskovits, M., *Surface-enhanced Raman spectroscopy: A brief retrospective*. Journal of Raman Spectroscopy, 2005. **36**(6-7): p. 485-496.
14. Billmann, J., G. Kovacs, and A. Otto, *Enhanced Raman effect from cyanide adsorbed on a silver electrode*. Surface Science, 1980. **92**(1): p. 153-173.
15. Otto, A., et al., *The "adatom model" of SERS (Surface Enhanced Raman Scattering): The present status*. Surface Science, 1984. **138**(2): p. 319-338.
16. Otto, A. and M. Futamata, *Electronic Mechanisms of SERS*, in *Surface-Enhanced Raman Scattering: Physics and Applications*, K. Kneipp, M. Moskovits, and H. Kneipp, Editors. 2006, Springer Berlin Heidelberg: Berlin, Heidelberg. p. 147-182.
17. Otto, A., et al., *Surface-enhanced Raman scattering*. Journal of Physics: Condensed Matter, 1992. **4**(5): p. 1143-1212.
18. Urban, A.S., et al., *Three-dimensional plasmonic nanoclusters*. Nano Letters, 2013. **13**(9): p. 4399-4403.
19. Xu, L., et al., *Nanoparticle assemblies: Dimensional transformation of nanomaterials and scalability*. Chemical Society Reviews, 2013. **42**(7): p. 3114-3126.

20. Garcia-Leis, A., J.V. Garcia-Ramos, and S. Sanchez-Cortes, *Silver nanostars with high SERS performance*. Journal of Physical Chemistry C, 2013. **117**(15): p. 7791-7795.
21. Boca, S., et al., *Flower-shaped gold nanoparticles: Synthesis, characterization and their application as SERS-active tags inside living cells*. Nanotechnology, 2011. **22**(5).
22. Fan, Z., et al., *Popcorn-shaped magnetic core-plasmonic shell multifunctional nanoparticles for the targeted magnetic separation and enrichment, label-free SERS imaging, and photothermal destruction of multidrug-resistant bacteria*. Chemistry - A European Journal, 2013. **19**(8): p. 2839-2847.
23. Lu, W., et al., *Gold nano-popcorn-based targeted diagnosis, nanotherapy treatment, and in situ monitoring of photothermal therapy response of prostate cancer cells using surface-enhanced raman spectroscopy*. Journal of the American Chemical Society, 2010. **132**(51): p. 18103-18114.
24. Lee, P.C. and D. Meisel, *Adsorption and surface-enhanced Raman of dyes on silver and gold sols*. Journal of Physical Chemistry, 1982. **86**(17): p. 3391-3395.
25. Khalili Fard, J., S. Jafari, and M.A. Eghbal, *A Review of Molecular Mechanisms Involved in Toxicity of Nanoparticles*. Adv Pharm Bull, 2015. **5**(4): p. 447-54.
26. Khlebtsov, N. and L. Dykman, *Biodistribution and toxicity of engineered gold nanoparticles: a review of in vitro and in vivo studies*. Chem Soc Rev, 2011. **40**(3): p. 1647-71.
27. Day, E.S., et al., *Nanoshell-mediated photothermal therapy improves survival in a murine glioma model*. J Neurooncol, 2011. **104**(1): p. 55-63.
28. Jawhari, T., A. Roid, and J. Casado, *Raman spectroscopic characterization of some commercially available carbon black materials*. Carbon, 1995. **33**(11): p. 1561-1565.
29. Sato-Berrú, R., et al., *Silver nanoparticles synthesized by direct photoreduction of metal salts. Application in surface-enhanced*

- Raman spectroscopy*. Journal of Raman Spectroscopy, 2009. **40**(4): p. 376-380.
30. Huang, H.H., et al., *Photochemical Formation of Silver Nanoparticles in Poly(N-vinylpyrrolidone)*. Langmuir, 1996. **12**(4): p. 909-912.
 31. Xu, G.-n., Qiao, Xue-liang, Qiu, Xiao-lin, Chen, Jian-guo, *Preparation and characterization of stable monodisperse silver nanoparticles via photoreduction*. Colloids and Surfaces A: Physicochemical and Engineering Aspects, 2008. **320**(1-3).
 32. Wang, P., et al., *Ag@AgCl: A highly efficient and stable photocatalyst active under visible light*. Angewandte Chemie - International Edition, 2008. **47**(41): p. 7931-7933.
 33. Muniz-Miranda, M. and G. Sbrana, *Evidence for Surface Ag⁺ Complex Formation by an Anion-Induced Effect in the SER Spectra of Phthalazine Adsorbed on Silver Sols*. Journal of Raman Spectroscopy, 1996. **27**(2): p. 105-110.